Oxide Engineering Using Metalorganic Aerosol Deposition

Alexander BELENCHUK[1], Sebastian HÜHN[2], Markus JUNGBAUER[2], Markus MICHELMANN[2], Oleg SHAPOVAL[1], Efim ZASAVITSKY[1], Vasily MOSHNYAGA[2]

[1]*IEEN "D. Ghitu", Academy of Sciences of Moldova, belenchuk@nano.asm.md*
[2]*I. Physikalisches Institut, Georg-August-Universitat-Gottingen, Germany,*

***Abstract* —Metalorganic aerosol deposition is shown to be one of the most promising techniques for the epitaxial growth of structurally perfect transition metal oxide films, superlattices and atomically layered oxides. The basics and the new developments of the technics are shortly descripted. Several new studies are presented to illustrate recent achievements of the technique. We demonstrate growth and properties of three different oxide systems: relatively thick thin films of optimally doped manganites - $La_{0.67}Sr_{0.33}MnO_3$ and $La_{0.67}Sr_{0.33}MnO_3$; ultra-short period superlattices - $(LaMnO_3)_n/(La_{0.5}Ba_{0.5}MnO_3)_{2n}$, which formed films of a "digital" manganite with near optimal level of doping; and metastable layered oxides - $Sr_{n+1}Ti_nO_{3n+1}$ films, which were formed via sub-unit cell control of epitaxy.**

***Index Terms* — epitaxy, metalorganic aerosol deposition, superlattices, thin films, transition metal oxides.**

I. INTRODUCTION

Perovskite-type complex transition metal oxides (TMO) display a remarkable spectrum of electronic, optical, and magnetic behavior: superconducting, ferroelectric, piezoelectric, and ferromagnetic properties are all accessible due to strong coupling between lattice, charge, spin and orbital degrees of freedom [1]. Extremely rich diversity of complex oxide functionalities is originated from a strong electronic correlation and can be further expanded by atomically tailored oxide heterostructures, which lead to emergent properties – e.g., superconducting interfaces between insulating oxides. This is why thin film preparation of TMO needs a thorough control at the nano- and even at atomic scale level.

The ability to grow perfect epitaxial films and artificial heterostructures is of critical importance both for fundamental understanding and following application of these materials. A number of growth techniques are currently employed to prepare thin film oxides. Common growth techniques include pulsed laser deposition (PLD) [2] and molecular beam epitaxy (MBE) [3]. Metalorganic chemical vapor deposition (MOCVD) technique require a volatile precursors, but in most cases the elements of TMO have precursors with a very low volatility (alkali earth elements) or even are non-volatile (rare earth elements). Due to the volatility problem, MOCVD of transition metal oxides is based on the injection of liquid solutions contained required precursors dissolved in an appropriate organic solvent [4].

The present study deals with one of the many variations of the liquid injection MOCVD technique that is Metalorganic Aerosol Deposition (MAD).

II. EXPERIMENTAL DETAILS

MAD is a solution-based chemical deposition technique that uses metal-chelate coordination compounds (e.g. La-, Sr-, Mn - acetylacetonates) as precursors dissolved in an organic solvent (e.g. dimethilformamide). Growth is performing by spraying of controllable volumes of the corresponding solutions onto the heated substrate. An oxide grows on the substrate as a result of heterogeneous pyrolysis reaction of the precursor molecules. The main distinctive feature of MAD technique from the other liquid injection ones is a unique combination of a high speed of aerosol motion (usually ≥ 20 m/s) with a very high temperature on the substrate surface (>800ºC). This combination allows of vapor phase creating in a very thin near-surface boundary layer even in the case of non-volatile precursors. Small thickness of boundary layer in combination with high pressures and high temperatures creates growth conditions controlled rather by mass transport than by surface kinetic.

The scheme of the MAD is shown in Fig. 1. To produce the high speed of aerosol flow we use a high pressure (> 5 bar) pneumatic nozzle. Six independent automated dosing units feed the nozzle by controllable volumes of different precursor solutions. Optical pyrometer and light scattering by aerosol are used for control of substrate temperature and aerosol flow intensity.

Ellipsometry is employed for *in situ* control of growth process. Incident polarized light passes a phase modulator with frequency ω, whereas detected light intensity varied with ω and 2ω. Measurements of intensities $I_\omega \sim \sin(2\psi)\sin(\Delta)$ and $I_{2\omega} \sim \sin(2\psi)\cos(\Delta)$ allow us to determine rotation ψ and phase shift Δ angles

independently from the absolute intensity. Fitting of ψ and Δ to suitable optical model yields information about film thickness, surface roughness and dielectric parameters of growing oxide film.

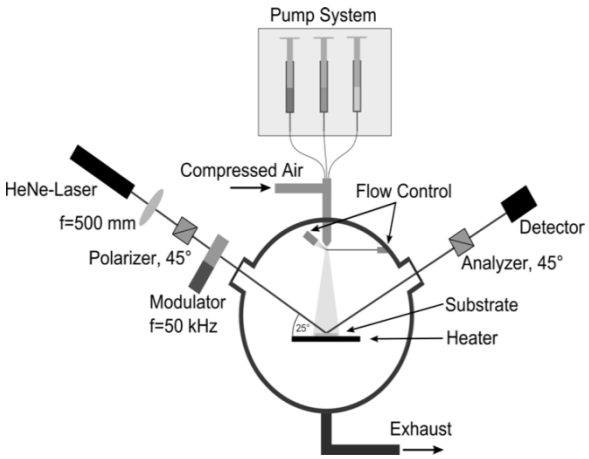

Fig. 1. Schematic diagram of the metalorganic aerosol deposition set-up equipped with ellipsometry.

All films, SLs and layered structures, presented in this study were grown on singly TiO_2 terminated STO (100) substrates. Surface morphologies were studied by scanning tunneling microscopy (STM) in Veeco Multimode V Scanning Probe Microscope. To determine overall thickness of the films as well as superlattice period we used a small-angle x-ray scattering (SAXS) in a Brucker D8 diffractometer, which was also employed for X-ray diffraction (XRD) analysis. Transport measurements were carried out on a Quantum Design PPMS platform. The magnetization as a function of temperature and magnetic field was measured using a Quantum Design MPMS SQUID magnetometer.

III. RESULTS

A. Thin films

The perovskite manganites, $La_{0.67}Sr_{0.33}MnO_3$ (LSMO) and $La_{0.67}Sr_{0.33}MnO_3$ (LBMO), have transition from a paramagnetic insulator to a ferromagnetic metal above the room temperature and possess near 100% spin polarization below the transition temperature. These properties make them perspective materials for spintronic application such as, for example, spin-dependent injection of carriers [5]. All applications require the growth of thin films with a device quality that is with an atomically smooth surface, a high Curie temperature, a large magnetization, and a low residual resistance.

In this study we report on the growth and properties of relatively thick LSMO and LBMO thin films grown by MAD technique and comparison of obtained results with the best results obtained by other techniques such as PLD and MBE.

Presented here the best functional properties of MAD grown films were obtained after a thorough optimization of all growth conditions: the growth temperature, composition of precursors, speed of deposition, and etc.

Fig. 2 shows an STM 1×1 μm image of a 23.7 nm thick LSMO film. The one-unit-cell-height steps and wide atomically flat terraces are clearly visible, pointing the "step-flow" mode of epitaxial growth. The absence of precipitates, related to the off-stoichiometric deposition, indicate an equal ratio between A- and B-cations.

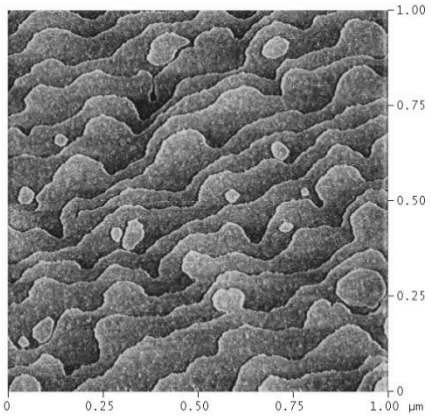

Fig. 2. STM image of 24 nm thick LSMO film grown on STO(100) substrate.

XRD analysis confirms epitaxial growth of uniformly strained manganite films. Near the substrate peaks we permanently observed a finite thickness fringes (Laue fringes) with the period corresponding well to the thickness of films, determined from SAXS.

The temperature-dependent resistivity of optimally doped LBMO and LSMO films are shown in Fig. 3. Metallic behavior for LBMO starts from T_{MI}=352 K, whereas LSMO has no evident metal-insulator transition up to 400 K, which is the maximum achievable temperature for our experimental setup. The dependence for LSMO looks like transition from one metal to another and, indeed, it is known that a high quality LSMO has transition from paramagnetic metal to ferromagnetic one without manifestation of the maximum on the R(T) curve.

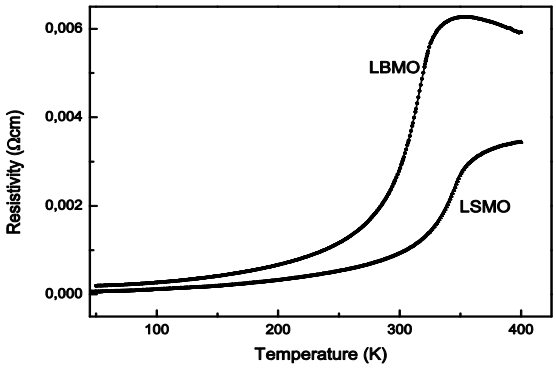

Fig. 3. Temperature-dependent resistivity of 59 nm thick LBMO and 24 nm thick LSMO films grown on STO(100) substrates.

Magnetic measurements showed the saturation magnetization at low temperature was equal to 3.2 and 3.5 μB/Mn for LBMO and LSMO, respectively. The Curie temperatures for these manganites are equal to 325 K for LBMO and 355 K for LSMO. The magnetization of both manganites is very soft with coercive field of only 30-40 Oe. This value reflects a high microstructural perfection (absence of pinning centers) in the materials.

The metal-insulator and magnetic transition temperatures as well as the values of magnetization are exactly coincided with the best result obtained for the films grown by PLD and MBE [5]. However, the residual low-temperature resistivity for our LSMO , which is only

35 μΩcm, is significantly smaller than the best value of 60 μΩcm for PLD grown films and do not inferior to the best value obtained for MBE grown films[5]. For LBMO we obtained the residual resistance of 120 μΩcm that is, to our knowledge, smaller than any previously published value.

Our results on the "bulk" manganite films epitaxy demonstrate the ability of vacuum-free MAD technique to produce films with superior functional properties required for device applications.

B. Digital superlattices

A-site disorder plays a fundamental role in the properties of manganites near the phase transitions. The ability thus to engineer disorder is critical both for fundamental science and for applications of correlated oxides. In this framework $(SrMnO_3)_n/(LaMnO_3)_{2n}$ superlattices (SLs) with a low number of unit cells $n\leq3$ have been intensively studied as a digitally ordered analog of the optimally doped LSMO [3]. From the other hand it is known that the half-doped LBMO can be synthesized as layer-ordered single crystal $(LaBa)Mn_2O_6$, due to greater A-cation mismatch than in LSMO. Therefore LBMO may give a good possibility to test the idea of digital ordering by SLs approach.

In this study we report on the MAD synthesis and properties of digital SLs of $(LaMnO_3)_n/(La_{0.5}Ba_{0.5}MnO_3)_{2n}$ with n=1-2, where the overall stoichiometry is equivalent to optimally doped LBMO.

As a prerequisite for the SLs growth, to obtain the half-doped manganite, a series of "bulk" LBMO thin films was grown with increasing Ba doping over the optimal level. Characterization of structural, magnetic and transport properties and their comparison with the phase diagram of manganites allows determining all conditions required for the half-doped LBMO synthesis.

The surface morphology of SLs consisted from a flat terraces covered by unit-cell-height islands, indicating thus a layer-by-layer mode of epitaxial growth.

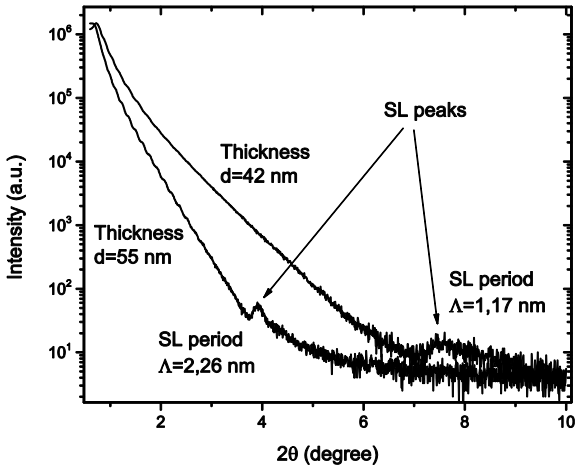

Fig. 4. SAXS patterns measured from the "digital" SL $(LaMnO_3)_n/(La_{0.5}Ba_{0.5}MnO_3)_{2n}$ on STO(100) with n=1 and 2.

In Fig. 4 we present the SAXS pattern of two $(LaMnO_3)_n/(La_{0.5}Ba_{0.5}MnO_3)_{2n}$ SLs with n=1 (33 periods) and 2 (25 periods). In spite of extremely short periods the SL peaks are clearly visible on the both curves, evidencing the formation of SL structures. The peak positions are very close to the desired SL periods, which are equal to 1.18 nm (3 unit cells) and 2.36 nm (6 unit cells) for n=1 and n=2, respectively. Due to a very small period the satellite SL peaks were not detected by XRD analysis for n=1, but for n=2 the SL^{-1} peak was clearly revealed. As in the case of "bulk" LBMO films, XRD shows clear Laue fringes with periods corresponded to the overall thickness, confirming thus formation of a coherently strained SLs.

For SL with n=1 the Curie temperature determined from the temperature dependence of magnetization is equal to 325 K, that is not so far from the "bulk" LBMO films. The saturation magnetization and coercive fields are also almost matched the values obtained for the "bulk" LBMO.

The temperature-dependent resistivity, shown in Fig. 5, reveals a metallic behavior starting from temperature of metal-insulator transition (T_{MI}). The SL with n=1 demonstrates values of T_{MI} and the temperature coefficient of the resistance, $TCR=(dR/dT)/R$, closer to optimally doped "bulk" LBMO films than SL with n=2. The residual resistance of 135 and 165 μΩcm, respectively for n=1 and n=2, confirms that a higher structural quality of "digital" material was obtained at a shorter SL period with n=1.

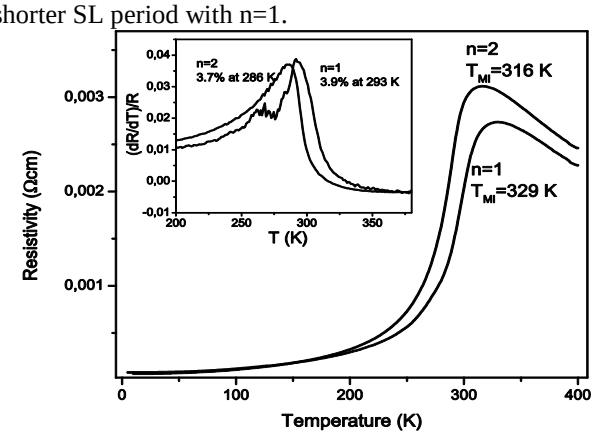

Fig. 5. Temperature-dependent resistivity of the digital SL $(LaMnO_3)_n/(La_{0.5}Ba_{0.5}MnO_3)_{2n}$ on STO(100). The inset shows temperature dependence of $TCR=(dR/dT)/R$.

The structural and functional properties of digitally synthesized LBMO are practically identical to the "bulk" thin film material. This result confirms the ability of MAD technique to produce extremely short period SLs, which can be applied to tailor properties of TMO.

C. Sub unit cell growth

Oxide engineering at the sub-unit-cell level can result in the creation of a new metastable material with enhanced or novel functionalities. To prove the ability of MAD for the atomic-level engineering we have grown the n=1–4 members of the layered superlattice-type $Sr_{n+1}Ti_nO_{3n+1}$ compounds. These metastable at $n\geq3$ compounds are known as Ruddlesden–Popper (RP) phases, which are built up with alternate stacks of rock salt SrO monolayers and perovskite $(SrTiO_3)_n$ block layers [3].

In this study we report on the MAD synthesis of RP phase by alteration of SrO and TiO2 monolayers with insertion an additional monolayer of SrO after n couples of $SrO\text{-}TiO_2$, i. e. we employed sub-unit-cell growth to

build up the whole of material, including $(SrTiO_3)_n$ block layers.

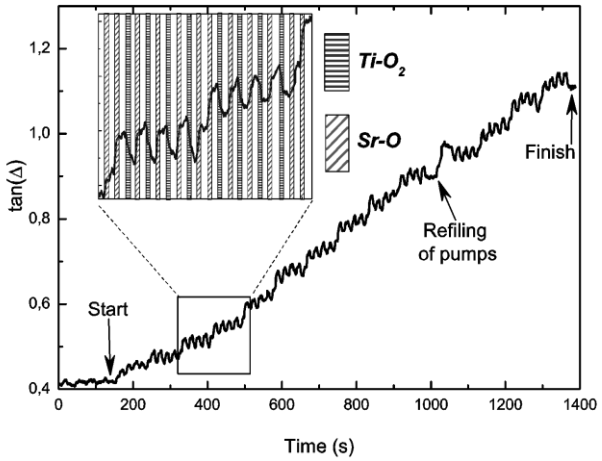

Fig. 6. *In situ* ellipsometric data for phase shift angle Δ during the growth of $Sr_5Ti_4O_{13}$ on STO(100) substrate.

The deposition process was controlled *in situ* via ellipsometry measurements. Ellipsometric monitoring of phase shift angle Δ, shown on Fig. 6, demonstrates that all separate steps of deposition can be identified. Increasing of tan(Δ) during deposition of SrO monoatomic layer and its decreasing at deposition of TiO_2 monoatomic layer leads to formation of oscillations, thus indicating a pure atomic layer-by-layer growth mode. Inserting of an additional SrO monolayer can be clearly identified as a couple of upward steps. The layer-by-layer mode of growth was also confirmed by STM analysis of surface morphology.

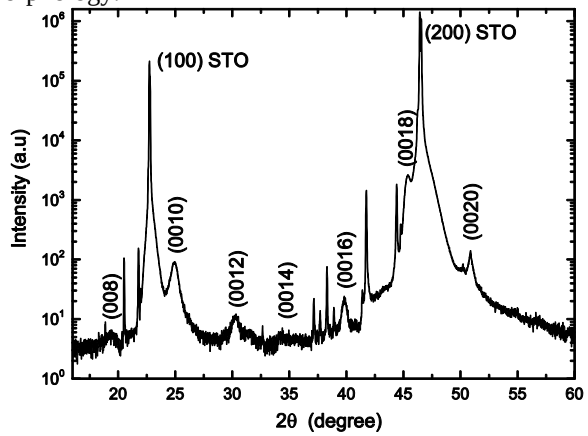

Fig. 7. XRD spectrum of $Sr_5T_4O_{13}$ epitaxial film grown on STO(100) substrate.

To prove the regularity in the periodicity of grown RP phases we performed XRD analysis. The *θ-2θ* XRD patterns in Fig. 7 confirm epitaxial orientation of film and formation of a new periodicity corresponded to specific value of $n = 4$ for the presented $Sr_5T_4O_{13}$ PR compound with total thickness equal to 25.1 nm according to SAXS measurements. All of the peaks denoted on the scan are at the correct *2θ* positions and correspond to c-lattice constant of 3.59(5) nm, which is approximate to the theoretic value of 3.6 nm, and corresponds to the total thickness of 7-periods films. Some broadening of peaks as well as weakness of (008) and (0014) peaks seems to be attributed for spotting non-periodicity in the stacking sequence.

This result demonstrates the ability of epitaxial engineering of metastable compounds by a sequential deposition of sub-unit-cell layers within the MAD technique. The growth oxides in any desired sequence with sub-unit-cell control offers a great potential for the tailoring of complex oxide properties required for different application.

IV. CONCLUSION

We have presented MAD growth and some properties of (1) optimally doped "bulk" LSMO and LBMO manganite thin films, (2) "digital" manganite films formed via ultra-shot period $(LaMnO_3)_n/(La_{0.5}Ba_{0.5}MnO_3)_{2n}$ SLs, and (3) films of metastable RP phase compounds formed via sub-unit-cell control of growth of $Sr_{n+1}Ti_nO_{3n+1}$ titanates . We have shown that the relatively simple and a vacuum-free MAD technique can produce films, SLs and even metastable atomically layered compounds of comparable quality to those grown by PLD or MBE.

REFERENCES

[1] J. M. Rondinelli and N. A. Spaldin, "Structure and Properties of Functional Oxide Thin Films: Insights From Electronic-Structure Calculations," *Advanced Materials*, vol. 23, no. 30, pp. 3363–3381, 2011.

[2] H. M. Christen and G. Eres, "Recent advances in pulsed-laser deposition of complex oxides," *Journal of Physics: Condensed Matter*, vol. 20, no. 26, p. 264005, Jul. 2008.

[3] D. G. Schlom, J. H. Haeni, J. Lettieri, C. D. Theis, W. Tian, J. C. Jiang, and X. Q. Pan, "Oxide nano-engineering using MBE," *Materials Science and Engineering: B*, vol. 87, no. 3, pp. 282–291, Dec. 2001.

[4] P. J. Wright, M. J. Crosbie, P. A. Lane, D. J. Williams, A. C. Jones, T. J. Leedham, and H. O. Davies, "Metal organic chemical vapor deposition (MOCVD) of oxides and ferroelectric materials," *Journal of Materials Science: Materials in Electronics*, vol. 13, no. 11, pp. 671–678, Nov. 2002.

[5] H. Boschker, M. Huijben, A. Vailionis, J. Verbeeck, S. van Aert, M. Luysberg, S. Bals, G. van Tendeloo, E. P. Houwman, G. Koster, D. H. A. Blank, and G. Rijnders, "Optimized fabrication of high-quality La0.67Sr0.33MnO3 thin films considering all essential characteristics," *Journal of Physics D: Applied Physics*, vol. 44, no. 20, p. 205001, May 2011.